ELSEVIER

Contents lists available at ScienceDirect

Microchemical Journal

journal homepage: www.elsevier.com/locate/microc



Selective separation and characterization of acylated and non-acylated anthocyanins via resin adsorption-desorption method

Anindita Paul ^{a,b}, Anirban Dutta ^{a,c}, Aditi Kundu ^a, Namita Banyal ^d, Gautam Chawla ^e, Anil Dahuja ^f, Supradip Saha ^{a,*}

- ^a Division of Agricultural Chemicals, ICAR-Indian Agricultural Research Institute, New Delhi 110012, India
- ^b ICAR-Central Tobacco Research institute, Rajahmundry 533105, India
- ^c National Institute of Secondary Agriculture, Ranchi, Jharkhand, India
- ^d Division of Floriculture, ICAR-Indian Agricultural Research Institute, New Delhi 110012, India
- ^e Division of Nematology, ICAR-Indian Agricultural Research Institute, New Delhi 110012, India
- ^f Division of Biochemistry, ICAR-Indian Agricultural Research Institute, New Delhi 110012, India

ARTICLE INFO

Keywords: Acylated Non-acylated anthocyanin Confocal microscopy Thermodynamics Macroporous resin Competitive adsorption

ABSTRACT

Anthocyanins, beyond offering a wide range of health benefits, they exist in both acylated and non-acylated forms. Purification of anthocyanins remains a significant challenge due to the presence of co-extractives viz. phenolics and sugars. Among tested resins, OPTIPORE L 493 demonstrated superior adsorption selectivity for -acylated anthocyanins (black carrot) over other phenolics. Whereas, in case of non-acylated anthocyanins (black rice), it effectively adsorbed both anthocyanins and phenolics. Sugars exhibited the highest desorption rate (62.2 %) due to the weakest adsorption on ion-exchange resins. Scanning electron microscopy (SEM) and confocal microscopy, confirmed that adsorption primarily occurred within the pore spaces of macroporous resins. The adsorption process followed the Freundlich isotherm model, indicating competitive adsorption for both acylated and non-acylated anthocyanins, as well as phenolics, but not for sugars ($R^2 > 0.901$, lowest χ^2 and AICc values, highest R_{adj}^2). Optimal adsorption of anthocyanins on DIAION HP 20 and OPTIPORE L 493 was observed at pH 6.0–7.0, with minimal influence of temperature variations on adsorption behavior. Thermodynamic analysis revealed that the adsorption process is endothermic, spontaneous, and random at the resin surface. By optimizing these adsorption variables, significant improvements in anthocyanin purity can be achieved.

1. Introduction

From last decade, the entire globe has witnessed an exploded growth in natural food colorant in nutraceutical industry which is the unique amalgam of pharmaceutical and food industries. Nonetheless, after COVID 19 pandemic there is a serious concern built up in production of natural immunity booster. Since then the global natural food colorant market excels in a new dimension which estimated to surpass \$ 3.66 billion by 2030, growing at a CAGR of 9.31 % from 2022 to 2030.

Apart from its use as natural colour it provides wide range of bioactivities including anti-cancerous properties. Anthocyanin is a very powerful antioxidant apart from its use as natural colorant.

In a natural anthocyanin rich extract, mainly phenolic compounds and carbohydrates lower the recovery of anthocyanin to the extent that it interferes with the biological activity of anthocyanin as well as its keeping quality [1,2]. Column chromatography became outdated technology due to several disadvantages viz., more laborious, time consuming, selective to small scale production etc. [3,4], whereas, production of natural colorant using counter current chromatography is not commercially feasible. Eventually, macroporous resin emerges as a cost effective replacement of existing sorbents with its several unique designs and features. The three-dimensional high molecular network of synthetic resins provides larger internal surface area which fasten adsorption process. In general, macroporous resins bind adsorbates through different mechanism like noncovalent bonding, van der Waals forces or hydrogen bonding, electrostatic forces etc. and get desorbed by selective solvents like methanol, ethanol or acidified water [5,6]. Macroporous resins generally used for the adsorption of phenolics, and the selection of a specific resin depends on the polarity of the phenolic compounds. Resin formed by polycondensation or polyaddition or

E-mail address: supradip.saha@icar.gov.in (S. Saha).

^{*} Corresponding author.

radical polymerization of styrene, acrylic acid, methacrylic acid, divinylbenzene or divinyl monomers are called adsorbent resin. Whereas, cross-linked porous spherical apolar resins when carry different functional groups through different treatments such as carboxylation, sulfonation, chlorormethylation followed by amination, they transformed into cation or anion exchange resins [7,8]. The use of surface-modified polystyrene divinylbenzene copolymers with different polar substituents in resins overcome pH instability under acidic or basic conditions which is one of the limitation of SPE sorbents [9]. Variable result of these resins are due to their properties such as porosity, particle size, functionality etc. Sadilova et al. [10] purified anthocyanins from black carrot, elderberry and strawberry sources using XAD-16 HP resins to remove sugars and salts, and at the same time to separate anthocyanin from phenolics Sephadex LH-20 adsorbent resin was used. In their experiments, anthocyanin purity was improved to 67.34 %. The thermodynamic interpretation such as free energy, entropy, enthalpy reveal different affinities towards resin and that in turn describe the sorption systems at equilibrium conditions [11,12-14]. Among limited studies, Buran et al. [5] reported that pseudo second order model and Langmuir isotherm model appeared to be best in describing the adsorption kinetics and mechanism of total phenolics and anthocyanin both from blueberry extracts on resins. In recent study by Belwal et al., [15] in their experiment proved that anthocyanin sorption under ultrasonic condition follow pseudo second order kinetics and multilayer adsorption on Amberlyst 15 (H⁺ form) resin. Lv and his team [16,17] reported that adsorption of honey flavonoid on AB-8 resin is best explained by Freundlich and Langmuir model at 25 °C whereas the thermodynamic parameters indicated that the adsorption process was exothermic. No study was explored on comparative sorption mechanism on resins among two different types of anthocyanins and other co-extractives. Anthocyanins present in nature as acylated and non-acylated form. In acylated anthocyanin, sugar is attached with the anthocyanidin, basic unit, connected with small acids viz. acetic, sinapic, caffeic, coumaric acids. Due to their chemical structure and nature, adsorption pattern of different group of compounds vary, which can be utilized for the purification purpose. Adsorption based purification using suitable resin is the key idea of the present study. Thus, developing a novel technology has significant benefits for the purification of anthocyanin from the crude extract using adorption/desorption processes. The study also aimed to understand the adsorption behavior and mechanism of acylated vs non-acylated anthocyanins. Optimized conditions (resin etc.) were focused to identify preferable adsorption of both type of anthocyanin compared to their co-extractives viz. sugars and other phenolics.

2. Experimental

2.1. Chemicals & apparatus

Seeds of black rice (Oriza sativa) and black carrot (Daucus carota ssp. sativus var. atrorubens) was obtained from the field of IARI, Pusa (28.080°N, 77.120°E). Commercially available adsorbent resin, DIAION HP 20 and ion exchange resin, OPTIPORE L 493 were procured from Sigma Aldrich Chemicals Pvt. Ltd. (Bangalore, India). Analytical reagent grade methanol and concentrated hydrochloric acid (≥36.5 %), sodium hydroxide (≥ 99 %) were procured from Merck Life Science Pvt. Ltd. (Mumbai, India). High-purity solvents for liquid chromatography, i.e., acetonitrile (ACN) and trifluoroacetic acid (TFA), were obtained from Merck Life Science Pvt. Ltd. (Mumbai, India). LC-MS grade methanol and formic acid were procured from Thermo Fisher Scientific India Pvt. Ltd. (Powai, Maharashtra, India). Deionized water with a resistivity of 18.2 m Ω .cm, prepared using a Millipore® water purification system, was used for all chromatographic analyses. Ultrasonicator bath (PCI Analytics, Thane, India), rotary evaporator (Laborota 4000, Heidolph®, Schwabach, Germany), Confocal Laser Scanning Microscopy (DM6000, Leica Microsystems, 195 Heidelberg, Germany), reciprocating shaker (SHIVAKITM, India) were used in the study.

2.2. Extraction of anthocyanins

Coarsely chopped black carrot and powdered black rice were used for extraction of anthocyanins. Extraction was carried out using methanol acidified with 0.1 % HCl, in a bath sonicator for 30 min, the process was repeated until the material became colorless [18]. The pooled extracts were then filtered and concentrated under vacuum in a rotary evaporator at 35 $^{\circ}\text{C}$ and 60 mbar, resulting in a viscous liquid. The extract was kept at -20 $^{\circ}\text{C}$ until analysis [19].

2.3. Quantification of anthocyanin, phenolics and sugars

Total monomeric anthocyanin content was assessed using the pH-differential method by recording absorbance at 530 and 700 nm using a spectrophotometer (Specord® plus-Analytik Jena AG, Germany) [20].

Total phenolic content was determined using a modified Folin-Ciocalteu (FC) method with gallic acid as the standard. A 0.25 mL aliquot of each sample or standard was diluted in 4 mL of water, followed by the addition of 0.5 mL of FC reagent. The mixture was allowed to react at room temperature for 3 min before adding 0.5 mL of 1 N sodium carbonate. The reaction proceeded for 1 h, after which absorbance was measured at 725 nm.

Total sugar content was determined following the procedures outlined by Gong et al. [21]. To be precise, the total sugar content was measured by adding 1 mL of anthrone reagent and $\rm H_2SO_4$ (5 mL; 96 %) in 0.1 mL of extract and 1 mL of distilled water were further added. Yellowish to orange colour was developed after placing in water bath for 20 min and intensity was measured at 490 nm.

2.4. Characterization by UPLC- QToF-ESI-MS/MS

Characterization of anthocyanins and phenolics present in the extract was executed by an ultra-performance liquid chromatographyhigh resolution mass spectrometer (UPLC-HRMS). UPLC data were acquired using Waters ACQUITY UPLC® systems equipped with a binary pump, an autosampler, a degasser, and a photo diode-array detector (PDA e λ). The chromatographic separation was performed on an ACQ-UITY UPLC C_{18} column (2.1 cm \times 100 mm, 1.8 μ m, Waters India Pvt. Ltd., Bangalore, India) at 20 °C. The mobile phase consisted of phase A: water (100 %) and phase B: methanol (100 %) with 0.1 % formic acid in both the phases. The mass data were acquired using a G2-XS QToF Mass spectrometer system equipped with an electrospray ionization (ESI) source and hybrid quadrupole-time-of-flight (QToF-MS) (Waters Corporation, Manchester, UK). The UPLC-QToF-MS system is controlled by the MassLynx 4.2 software.

2.5. Activation of commercial resins

Prior to use, the macroporous resin, DIAION HP 20 was soaked in ethanol (95 %) for 1 h and washed thoroughly with distilled water. OPTIPORE L 493 was immersed in 1 N NaOH for 1 h followed by rinsing with distilled water until it became neutral. Then it was rinsed again with distilled water after soaking in 1 N HCL for an hour. Resins were ready after drying at 60 °C. The moisture content was subsequently determined and all calculation was performed based on the weight of the dry resin.

2.6. Sorption study

2.6.1. Static adsorption/desorption study

Pre-screened activated DIAION HP 20 and OPTIPORE L493 resins underwent batch adsorption studies to evaluate the effects of adsorbent quantity and contact time at ambient temperature (28 °C) on anthocyanin sorption. To assess the influence of contact time, 0.125 g of dry resin was equilibrated with 5 mL aqueous (pH 3.5) crude extracts of black carrot (500 μ g mL⁻¹) and black rice (5000 μ g mL⁻¹) separately in a

30 mL tube, shaken at 120 rpm for 0.16 to 24 h. OPTIPORE L493 was tested at 0.0625–0.25 g per 5 mL extract at optimized equilibrium times of 2 h and 8 h for acylated black carrot and non-acylated black rice, respectively. DIAION HP 20 resin was tested at 1 h and 4 h under similar conditions. After adsorption, the supernatant was quantified for anthocyanin content using spectrophotometer at 520 nm.

Desorption of anthocyanin from the resins were carried out in the same tubes after attainment of adsorption equilibrium. A certain amount (2 mL) of the supernatant was separated and replaced with same volume of fresh buffer of pH 3.5 into each tubes and kept in shaker for respective equilibrium time at same temperature. The supernatant was syringe filtered and anthocyanin concentration was estimated in the similar way described earlier.

The amount adsorbed, q_e (μg g^{-1}) and % adsorption, A (%), the % desorption of the resins, D (%), was estimated with following eq. (1), (2) and (3)

$$q_e = \frac{(C_0 - C_e)}{W} \times V \tag{1}$$

$$A(\%) = \frac{(C_0 - C_e)}{C_0} \times 100 \tag{2}$$

$$D(\%) = \frac{(5C_d - 2C_e)}{5(C_o - C_e)} \times 100 \tag{3}$$

where, C_0 and C_e represent the initial and equilibrium liquid-phase concentrations ($\mu g \ mL^{-1}$), respectively, V stands for the volume of solution (mL), and W denotes the weight of dry resins (g). C_d indicates the concentration of anthocyanins in desorption solution ($\mu g \ mL^{-1}$).

2.6.2. Adsorption isotherm

To predict the adsorption mechanism for both anthocyanin, phenolics and sugar at isotherm condition adsorption study was carried out for black rice and black carrot anthocyanin rich extract on both the resins. A pre-weighed amount of both the resins (250 mg of DIAON HP-20, 62.5 mg of OPTIPORE L-493) were added into 5 mL crude extracts of varying concentrations (200–1000 mgL $^{-1}$ for black carrot, 4000–12,000 mgL $^{-1}$ for black rice). Adsorption was conducted at 25 \pm 3 $^{\circ}$ C in a shaker at 120 rpm. The equilibrium adsorption isotherms for anthocyanins, other phenolics, and sugars were determined using following equations.

Freundlich isotherm

$$q_e = K_f C_e^{1/n} \tag{7}$$

Langmuir isotherm

$$q_{e} = \frac{Q_{0} K_{L} C_{e}}{1 + K_{L} C_{e}}$$
 (8)

Temkin isotherm

$$q_e = \left(\frac{RT}{b}\right) \ln(AC_e)AC_e \tag{9}$$

Dubinin-Radushkevich isotherm:

$$lnq_{e} = lnq_{m} - K\varepsilon^{2}$$
(10)

Elovich isotherm

$$\ln \frac{q_e}{C_e} = \ln K_e q_l - \frac{q_e}{q_l} \tag{11}$$

where C_e (µg mL⁻¹) represents the equilibrium concentration, q_e (µg g⁻¹) signifies the adsorption amount at equilibrium, Q_0 stands for the maximum adsorption capacity (mg g⁻¹), K_L is the affinity constant in Langmuir model. K_F and n are the Freundlich constants where, K_F represents the adsorption capacity and n denotes the adsorption intensity. A (mL g⁻¹) represents the Temkin isotherm equilibrium binding constant, n b (J mol⁻¹) signifies constant associated with the heat of sorption, n

stands for universal gas constant (8.314 J mol $^{-1}$ K $^{-1}$), T represents the temperature (308 K) and B is the Temkin isotherm constant. q_m (µg g $^{-1}$) denotes the theoretical monolayer adsorption capacity, K (mol 2 J $^{-2}$) stands for the coefficient of activity related to the mean sorption energy and ϵ represents Polanyi potential. Whereas, K_e is related to Elovich constant and q_1 indicates Elovich maximum adsorption capacity.

2.6.3. Desorption experiment

An aliquot of 3 mL of each extract was taken out from adsorbed screened resins viz., DIAON HP-20 and OPTIPORE L-493 and were replaced by the same volume of pH 3.5 buffer solution followed by agitation at 120 rpm at a controlled temperature $25\pm2\,^{\circ}\mathrm{C}$ for respective equilibration time. After achieving of adsorption equilibrium, the aliquot of the desorbed extract from respective resins were taken out and quantified the concentration of anthocyanins and phenolics in the desorption solution.

2.6.4. Dynamic adsorption

A dynamic adsorption experiment was conducted with the best performing resin through a dynamic test for crude anthocyanin extract of black carrot and black rice separately, he hydrated resin was packed into a glass column measuring 35 cm in length and 3.0 cm in internal diameter, with a bed volume (BV) of 20 mL. Each anthocyanin-rich crude extract (15 mL) was loaded onto the column separately, up to the resin's saturation capacity (where the anthocyanin concentration in the exit solution reached approximately 5 % of the inlet concentration). The setup was shielded from direct light and allowed to equilibrate for a specified duration. Following equilibration, the column was thoroughly washed by passing of 3 BV of deionized water in each cycle. The washing process was continued until the elute tested negative with Fehling's solution confirming the removal of unadsorbed sugars and other compounds. Adsorbed compounds were eluted with acidified ethanol, and the eluate was concentrated using a rotary evaporator to remove ethanol completely. The resulting residue was lyophilized to obtain purified, anthocyanin-rich powder. The concentration of anthocyanins in the extracts before and after adsorption was analyzed using spectrophotometer.

2.7. Characterization of macroporous resins

2.7.1. Scanning electron microscopy (SEM)

The microstructures of both the adsorbent and ion exchange resins were visualized using a scanning electron microscope (Tescan Vega-3 LMU, Brno-Kohoutovice, Czech Republic). Specifically, resins particles were mounted onto an aluminium stub and then sputter-coated with a layer of gold/palladium alloy. The samples were examined using SEM set at 15 kV. The appearance of resins was visualized under SEM at magnifications of 20,000 and 50,000 times.

2.7.2. Confocal microscopy

The unadsorbed and adsorbed DIAION HP 20 and OPTIPORE L 493 resins for both type of anthocyanins were examined using a confocal laser scanning microscope (DM6000, Leica Microsystems, 195 Heidelberg, Germany). An Argon laser diode at 405 nm was used for FITC fluorescence, with an excitation filter (EMP) at 413 nm and an emission filter (EMP) at 550 nm. Gain settings were set at 100 for FITC and 800 for Alexa Fluor 594 to maintain consistent fluorescence signal comparisons. The pinhole aperture was adjusted to 90.05 μm for both FITC and Alexa Fluor 594. Images were captured using a $10\times$ dry objective with variable zoom settings, ensuring that fluorescence signals from FITC and Alexa Fluor 594 were acquired simultaneously at the same depth, focus, and magnification. The images were merged using LAS AF software (Leica). Bright-field images were taken with an EA Prime inverted microscope (Leedz Microimaging Ltd., Leeds, UK) and analyzed using LMI Image Analysis software

2.7.3. Brunauer-Emmett-teller (BET) surface area measurement

The BET surface areas of the adsorbent were measured using Demo Autoflow, 2020 Anton Paar GmbH (Anton Parr) surface area analyzer where N_2 gas was used as adsorbate. Prior to measurement, the adsorbent was degassed at 100 $^{\circ}\text{C}$ at 20 $^{\circ}\text{C}$ min $^{-1}$ for 60 min.

2.8. Statistical analysis

All treatments and analyses were carried out in triplicate. The data were presented as mean \pm standard deviation (SD) values. Statistical analysis was executed using SPSS 16.0 (SAS Institute, Cary, NC, USA). The significance of differences between variables was evaluated through one-way ANOVA. *P*-values below 0.05 were deemed statistically significant, and the Tukey-Kramer HSD comparison test was employed to distinguish mean differences.

3. Results and discussion

3.1. UPLC-HRMS based characterization of anthocyanins

Using the accurate molecular masses and MS/MS fragmentation patterns, the constitutive anthocyanins present in the purified extracts of black rice and black carrot were successfully identified. Twelve compounds in black rice, and 18 compounds in black carrot were tentatively identified well within the approximate mass error value (Δ m/z) of ± 3 ppm (Tables 1 & 2).

In the black rice extract, the predominant anthocyanidins and their glycoside derivatives viz. petunidin, cyanidin, peonidin, malvidin, cyanidin-3-gentiobioside, cyanidin 3-hexoside, peonidin 3-hexoside and malvidin 3-pentoside were tentatively identified at t_R of 26.52, 29.15, 31.25, 33.32, 4.57, 4.68, 6.56 and 16.94 min, respectively with their corresponding protonated molecular ion $[M + H]^+$ peaks at m/z of 318.0736, 288.0635, 302.0793, 331.0813, 612.1691, 450.1156, 464.1312 and 464.1333 (Table 1). Therefore, black rice is considered as another source of non-acylated anthocyanins [18].

In black carrot extract, apart from few free anthocyanidins, the major anthocyanins detected were acylated forms of glycosides (Table 2). Cyanidin-3-O-xylosyl-feruloyl-glucosyl galactose, cyanidin-3-O-xylosyl-synapoyl-glucosyl galactose, cyanidin-3-galactosyl coumaryl glucoside, peonidin-3-O-xylosyl glucosyl galactoside, and cyanidin-3-O-feruloyl galactosyl-glucoside were eluted at t_R of 3.93, 4.19, 18.77, 21.95 and 32.56 min with their respective protonated adducts of molecular ion [M + H] $^+$ at m/z 920.2575, 950.2682, 756.1965, 758.2231, 788.2116 and 288.0620. Fragmentation pattern of the molecular ions confirmed the identities of the major compounds e.g., cyanidin-3-galactosyl coumaryl glucoside was identified from the fragmentation of the molecular ion to the daughter ion peaks at m/z 594.1409 and 288.0630 due to liberation of one glucose moiety (162 amu) and characteristic protonated ion of

cyanidin unit, respectively. Both mono-acylated di- and tri-glucosides were present in the black carrot extract with major acyl groups originating from ferulic, sinapic and coumaric acid.

3.2. Equilibrium time for adsorption

The batch adsorption study was conducted to determine the equilibrium time for both DIAION HP 20 and Optipore L493, using black carrot and black rice anthocyanin extracts. Fig. S1 illustrates the adsorption percentage of both the anthocyanins on both the resins. Initially, the rate of adsorption was faster for both resins with acylated anthocyanin, reaching its peak within the first 2 h. Following this, the adsorption rate significantly slowed for adsorbent resin over the next 2 h, stabilizing by 24 h. For Optipore L 493, adsorption was faster in the first hour, then slowed over the next 24 h.

In the case of black rice anthocyanin, Diaion HP20 achieved full stability after 8 h, with the highest rate of adsorption occurring in the first hour., whereas, in case of Optipore L493, it reached stability after 4 h of adsorption.

Therefore, the equilibrium time for black carrot anthocyanin was decided to be 2 h for Diaion HP 20 and 1 h for Optipore L 493. For black rice, equilibrium was 8 and 4 h for Diaion HP 20 and Optipore L 493, respectively. After equilibrium, only a 2–3 % increase in adsorption was observed. With the same amount of resin, the adsorption pattern followed this order: acylated anthocyanin on ion exchange resin > nonacylated anthocyanin on ion exchange resin > acylated anthocyanin on adsorbent resin. Optipore L 493 exhibited faster adsorption compared to the other resin for both types of anthocyanin.

3.3. Equilibrium amount of sorbents

For determination of equilibrium amount of sorbent (resin), variable amount of resin was used to evaluate the anthocyanin sorption efficiency and the same is presented in Fig. S2. Result demonstrated that as the quantity of resin increased, the adsorption capacity decreased; however, there was an increase in the percentage of sorption. At 0.25 g of adsorbent resin for both type of anthocyanin, maximum sorption (%) was recorded as 94.20 % for acylated anthocyanin and 81.47 % for nonacylated anthocyanin. Whereas, it was 0.0625 g for ion exchange resin in case of both type of anthocyanins. The resin provided maximum adsorption (%) of 84.22 % for acylated anthocyanin and 70.16 % for non-acylated anthocyanin. Hence, 0.25 g of adsorbent resin and 0.0625 g of ion exchange resin was selected for both type of anthocyanin during further experimentation. The amount was finalized after further experimentation with enhanced amount of adsorbents and it was recorded that only 10-15 % variation was observed even after 2-4 times enhancement of the dose of sorbent especially for ion exchange resin.

Table 1Identification of anthocyanins present in resin purified ethanolic extract of black rice by HRMS-ESI-QTOF-MS.

t _R (min)	Compounds	Chemical formulae	Neutral or exact mass (Da)	Observed mass ${}^{a}[M + H]^{+}(m/z)$	Mass error (Δ m/z, ppm)	MS/MS fragments
4.19	Cyanidin-dihexoside	$C_{27}H_{31}O_{16}$	610.1534	611.1609	-0.49	431.0978, 288.0630, 251.0345, 181.0717
4.57	Cyanidin-3- gentiobioside	$C_{27}H_{31}O_{16}$	611.1616	612.1691	-0.49	343.1242, 270.0532, 288.0632
4.68	Cyanidin 3-hexoside	$C_{21}H_{21}O_{11}$	449.1084	450.1156	-1.33	269.0448, 288.0630, 252.04266, 181.0711
6.56	Peonidin 3-hexososide	$C_{22}H_{23}O_{11}$	463.1241	464.1312	-1.51	302.0789, 283.0606, 181.0717
16.94	Malvidin 3-pentoside	$C_{22}H_{23}O_{11}$	463.1241	464.1333	3.02	332.0891, 151.0604, 133.0506
26.52	Petunidin	$C_{16}H_{13}O_{7}$	317.0656	318.0736	0.63	301.0707, 284.0673, 267.0654, 253.0494
29.15	Cyanidin	$C_{15}H_{11}O_6$	287.0556	288.0635	0.35	271.0603, 255.0656, 239.0704, 223.0759
31.25	Peonidin	$C_{16}H_{13}O_{6}$	301.0712	302.0793	0.99	285.0760, 268.07356, 251.07083, 220.0529
33.32	Malvidin	$C_{17}H_{15}O_7$	331.0813	332.0896	1.51	315.0863, 281.08097, 264.0787
34.60	Malvidin 3-hexoside	$C_{23}H_{25}O_{12}$	493.1346	494.1429	1.01	332.08917, 314.0793, 181.0712, 163.0612
36.33	Cyanidin 3-pentoside	$C_{20}H_{19}O_{10}$	419.0979	420.1066	2.14	288.0634, 270.05293, 151.0602, 133.0502
36.77	Petunidin 3-hexoside	$C_{22}H_{23}O_{12}$	479.1190	480.1277	1.87	163.0614, 318.0736, 300.1334, 181.0716

Table 2 Identification of anthocyanins present in resin purified ethanolic extract of black carrot by HRMS-ESI-QTOF-MS.

t _R (min)	Compounds	Chemical formulae	Neutral or exact mass (Da)	Observed mass ${}^{a}[M+H]^{+}$ (m/z)	Mass error (Δ m/z, ppm)	MS/MS fragments		
3.93	Cyanidin-3-O-xylosyl-feruloyl-glucosyl galactose	$C_{42}H_{47}O_{23}$	919.2508	920.2575	-1.24	726.2003, 590.1423, 288.0632, 195.0654,		
4.19	Cyanidin-3-O-xylosyl-synapoyl-glucosyl galactose	$C_{43}H_{49}O_{24}$	949.2614	950.2682	-1.05	726.2004, 288.0630, 225.0760, 181.0712		
16.11	Peonidin-3-O-(di succinyl glucoside)	$C_{30}H_{31}O_{17}$	663.1639	664.1738	3.10	484.1084, 302.0792, 181.0710, 119.0343		
16.38	Dimer of malvidin & petunidin-3-O-glucoside	$C_{39}H_{38}O_{19}$	810.2007	811.2087	0.21	631.1452, 318.0733, 332.0890, 181.0712		
16.68	Petunidin	$C_{16}H_{13}O_{7}$	317.0656	318.0740	1.89	301.0705, 284.0672, 267.0653, 253.0490		
18.77	Cyanidin-3-galactosyl coumaryl glucoside	$C_{36}H_{35}O_{18}$	755.1862	756.1965	3.24	594.1409, 288.0630, 181.0710, 165.0552		
21.95	Peonidin-3-Oxylosyl glucosyl galactoside	$C_{33}H_{41}O_{20}$	757.2152	758.2231	0.12	578.1595, 398.0964, 318.0730,		
22.34	Peonidin	$C_{16}H_{13}O_6$	301.0712	302.0799	2.98	285.0762, 268.0735, 251.0707, 220.0523		
24.72	Malvidin	$C_{17}H_{15}O_7$	331.0813	332.0883	-2.41	315.0863, 281.0806, 264.0783		
26.62	Cyanidin-3-O-xylosyl-glucosyl galactoside	$C_{32}H_{39}O_{20}$	743.1996	744.2068	-0.81	564.1440, 414.0913, 288.0631, 181.0712		
28.73	Peonidin-3-glucoside	$C_{22}H_{23}O_{11}$	463.1240	464.1307	-2.50	302.0799, 283.0603, 181.0712		
29.03	Delphinidin-3-O-rutinoside	$C_{27}H_{31}O_{16}$	611.1612	612.1689	-0.21	327.1293, 304.0582, 286.0473		
30.54	Cyanidin-3 xylosyl galactoside	$C_{26}H_{29}O_{15}$	581.1506	582.1471	-2.23	432.0958, 288.0631, 181.0712		
32.36	Delphinidin	$C_{15}H_{11}O_{7}$	303.0500	304.0578	0.00	287.0550, 270.0523, 253.0496, 236.0463		
32.56	Cyanidin-3-O- feruloyl- galactosyl-glucoside	$C_{37}H_{39}O_{19}$	787.2047	788.2116	-1.14	608.14912, 288.0631, 195.0653, 181.0712		
32.71	Cyanidin	$C_{15}H_{11}O_6$	287.0551	288.0620	-3.12	271.0602, 255.0654, 239.0706, 223.0754		
39.07	Dimer of malvidin-3-O-glcoside & delphinidin-3-O-glucoside	$C_{44}H_{46}O_{24}$	958.2379	959.2450	-0.76	779.1820, 599.1187, 332.0890, 304.0577		
39.66	Dimer of malvidin-3-O-glucoside & peonidin-3-O-glucoside	$C_{45}H_{48}O_{23}$	956.2586	957.2672	0.80	777.2031, 597.1394, 332.0890, 302.0795		

The amount of ion exchange resin needed lesser to reach equilibrium compared to adsorbent resin for both type of anthocyanin.

3.4. Comparative adsorption isotherm of anthocyanin, phenolics and sugar

Comparative adsorption efficiency of anthocyanin, phenolics and sugars were carried out for both black rice and black carrot anthocyanin on DIAION HP 20 and OPTIPORE L 493 (Table 3). Data was fitted into different isotherm models and constants of those models were enlisted in Table 4, Table S_1 , S_2 .

DIAION HP 20 performed well for black carrot anthocyanin with 93.2 % adsorption. In comparison to anthocyanin, phenolics in black carrot also adsorbed with good adsorption value (95.2 %) on the same resin surface. In contrast, sugars present were poorly adsorbed with

Table 3Comparative sorption of anthocyanin, phenolics and sugar for acylated and non-acylated sources on adsorbent and ion exchange resins.

	% Adsorption								
Resin	Crude Extract	Anthocyanin	Phenolics	Sugar					
DIAION HP 20	Black carrot)	93.2 ± 0.42^{b}	95.2 ± 0.32^{c}	44.2 ± 0.54^{a}					
	Black rice	81.8 ± 0.09^{c}	$92.9 \pm \\ 0.02^{a}$	$\begin{array}{l} 40.9 \pm \\ 3.28^{b} \end{array}$					
OPTIPPORE L- 493	Black carrot	92.3 ± 0.30^{b}	$9.3\pm0.33^{\text{a}}$	$10.9 \pm \\3.31^a$					
	Black rice	77.1 ± 0.22^{c}	$\begin{array}{l} 87.8 \pm \\ 0.03^a \end{array}$	$\begin{array}{l} 70.9 \pm \\ 1.82^b \end{array}$					

Rows sharing same letter are not significantly different (p < 0.05); Result based on mean of three determinations, significance level checked at 5 % by Tukey compare mean test

maximum efficiency of 44.2~%. In case of black rice anthocyanin, DIA-ION HP 20 was quite good in adsorbing anthocyanin (81.8 %) but per cent adsorption of phenolics was more and it was 92.9 %. Similarly, adsorption for sugars were 40.9 %.

In case of OPTIPORE L 493, 92.3 % adsorption was recorded for black carrot anthocyanin. On contrary to DIAION HP 20, poor adsorption was recorded in case of both phenolics (9.3 %) and sugars (10.9 %). In case of black rice, adsorption of anthocyanin and phenolics by OPTIPORE L 493 were 77.1 % and 87.8 %. Interestingly, adsorption of sugars was in the range of 70.9 %.

Before the start of the experiment, phenolics (other than anthocyanins) were also estimated in the black rice and black carrot extract. And it was more in case of black rice. On DIAION HP 20 resin, both the anthocyanins and phenolics were well competitive during adsorption. As in black rice, phenolics content is more, and due to smaller in size as compared to anthocyanins, they get more chance to occupy the adsorption site of both the resins compared to non-acylated anthocyanin. On the other hand, in black carrot, adsorption efficiency of anthocyanins were significantly more than phenolics and it might be attributed to better ionic interaction of flavylium cation of anthocyanidin coupled with the amount of molecules present. This will prove to be advantageous during purification of anthocyanins.

The different isotherm models were presented in Fig. S1, S2 and S3. The coefficient of determination (R^2) in Table 4, S1 and S2 depicted that Freundlich model fitted well for both type of anthocyanin $(R^2=0.848-0.956)$ adsorption on both type of resins $(R^2=0.924-0.997).$ In case of phenolics, Freundlich model fitted well $(R^2=0.884-0.965)$ for both the sources on both the resins except black carrot on DIAION HP 20. In case of sugars from both sources also, Freundlich model $(R^2=0.773-0.900)$ best explained the adsorption on OPTIPORE L 493 but not on DIAION HP 20. For both anthocyanin sorption on both the resins, the values of adsorption intensity (1/n) value being less than 1, indicate that the adsorption process was favourable for anthocyanin. Whereas, in case

Table 4

Different adsorption isotherm parameters for anthocyanin adsorption of acylated and non acylated sources on adsorbent and ion exchange resins.

			Freundlich model		Langmuir model		Temkin model			Dubinin- adushkevich model		Elovich model			
Resins	Source	1/n	K _f	K _f . 1/n	R ²	Kı	R ²	A	В	b	R ²	E	R ²	K _e	R ²
DIAION HP 20	Black carrot	0.806	583.714	470.473	0.956	80	0.682	0.194	5362	0.478	0.955	158.114	0.890	1.000	0.517
	Black rice	0.683	2.202	1.504	0.848	700	0.894	0.013	20,613	0.12	0.926	7.955	0.986	1.002	0.471
OPTIPORE-L 493	Black carrot	0.948	1081.35	660.06	0.890	300	0.089	0.138	34,827	0.074	0.971	129.09	0.958	1.000	0.003
	Black rice	0.610	1804.679	3712.056	0.929	1100	0.911	0.010	174,748	0.015	0.962	6.482	0.981	1.000	0.690

of phenolics adsorption on OPTIPORE L 493, the slope (1/n) values is less than unity except black carrot. It signifies that the adsorption of anthocyanin and phenolics on resins follows L-type isotherms (Figure S₁ and S₂). On the contrary, the 1/n values for both sources sugars adsorption on both resin is more than unity predicts the adsorption process was not favourable for sugars except for non acylated source on OPTIPORE L 493 ion exchange resin (Figure S₃). The K_f·1/n value for acylated anthocyanins is more for OPTIPORE L-493 (660.06) than DIAION HP 20 (470.47), whereas, for non-acylated anthocyanin, the similar trend follows: OPTIPORE L 493(3712.06) > DIAION HP 20 (1.50) (Table 4). In case of phenolics adsorption, similar trend follows for black rice phenolics viz., OPTIPORE L 493(14,961,99) > DIAION HP 20 (1491.77) but opposite trend follows for black carrot phenolics viz., OPTIPORE L 493(1.63) < DIAION HP 20 (170.18) (Table S₁). On the other hand, Kf1/n value for all sources sugar are well below than the values for anthocyanin and phenolics and the trends follow similar like phenolics adsorption viz., for black rice: OPTIPORE L 493(13700) > DIAION HP 20 (2.25) and for black carrot OPTIPORE L 493(10.18) < DIAION HP 20 (21.39) (Table S2). Based on K61/n values, highest adsorption capacities obtained by OPTIPORE L 493 in adsorbing both type of anthocyanin and phenolics of non-acylated source, whereas, DIAION HP 20 resin obtained maximum K_f·1/n value for adsorbing phenolics of acylated source. The better fitting Freundlich model assured that competitive adsorption took place between phenolics and anthocyanin. Acylated sourced phenolics were poorly adsorbed on OPTIPORE ion exchange resins probably due to several reasons such as phenolics are not charge bearing compounds and due to comparative lesser content in acylated source contributes lesser in competitive adsorption. The Temkin isotherm model also implies that acylated anthocyanin is strongly bind to both the resins compared to its phenolics, whereas, non-acylated source phenolics is strongly bind to resins compared to non-acylated anthocyanins (especially on ion exchange resin).

The Figure S_1b , S_2b and S_3b revealed that the adsorption of nonacylated anthocyanin on both the resins do follow the Langmuir model as the correlation coefficients are sufficiently good but acylated anthocyanin on both the resins do not follow at all (Table 4). On the other hand, Langmuir model was well fitted for phenolics adsorption on both type of resins in case of non-acylated anthocyanin source but it is not fitted at all for acylated source phenolics on any of the resins (Table S_1) On the contrary, sugars of none of the sources fitted well in Langmuir model (Table S_2). It also depicts that the observed monolayer sorption capacity was significantly lower than their adsorption at equilibrium especially for black carrot phenolics and sugar on both the resins.

From Figure S_1c , S_2c and S_3c it can be extrapolated that the Temkin model can well explain the adsorption behavior of both type of anthocyanin on both type of resins. Similarly, this model also can well explain the phenolics adsorption on both type of resins except black carrot derived phenolics on OPTIPORE L 492 resins. At the same time this model cannot well explain the sugar adsorption on both type of resins. It

also affirms from Table 4 that heat required for sorption of both type of anthocyanin, both sources of phenolics other than anthocyanins and sugar on ion exchange resin is quite lesser than on adsorbent resins except black carrot sugar (Table S₁ and S₂). It implies that both type of anthocyanin is strongly bind on adsorption site of ion exchange resin than on adsorbent resins. Interestingly, black rice phenolics have lesser heat of adsorption than its non-acylated anthocyanin on both adsorbent and ion exchange resins. On the contrary, black carrot phenolics have more heat of adsorption than its acylated anthocyanin on both adsorbent and ion exchange resins. On the other hand, heat of adsorption for sugars of acylated source anthocyanin is quite lesser than phenolics adsorption on DIOAN HP 20 adsorbent resins, whereas heat of adsorption value for sugars of non-acylated source anthocyanin is equal with their phenolics. On the contrary, both sources sugars acquired more heat of adsorption than their anthocyanin and other phenolics on OPTIPORE L 493 resin.

Table 4, S_1 and S_2 revealed that the adsorption of both type of anthocyanin on any of the resins cannot be described well by Elovich isotherm model (Fig S_1 d, S_2 d, S_3 d). On the contrary, adsorption of both sources phenolics on both of the resins exhibits a good fit with the Elovich model. At the same time, adsorption of none of the sources sugar on both the resins cannot be described by Elovich model.

The Fig S₁e, S₂e, S₃e and Table 4, S₁ and S₂ depicts that the Dubinin–Radushkevich model is well fitted for adsorption of both type of anthocyanin on both adsorbent and ion exchange resins. The model is quite well fitted in explaining adsorption of phenolics too but not any of the sources sugar on any type of resins. This model again proves that the mean sorption energy for adsorption of acylated anthocyanin on both type of resins predicts particle diffusion may predominant at its adsorption site (as $E > 16 \text{ kJ mol}^{-1}$). Additionally, for phenolics also, acylated anthocyanin source-phenolics sorption on both type of resins, E value recorded more than 16 kJ mol⁻¹, whereas non-acylated anthocyanin source-phenolics sorption on both type of resins, E value is below 8 kJ mol⁻¹. On the contrary, E value lies below 8 kJ mol⁻¹ for adsorption of sugars of both the sources on both type of resins.

For further optimization of adsorption isotherm data of anthocyanin, phenolics and sugars, the comparative effectiveness of the different models in explaining the data was evaluated based on $R^2_{Adj,}\,SSE$ and chi-square. The ability of all models to establish correlations is depicted in Table S_3 where the values were employed to assess and gauge the performance of the models. Moreover, for better prediction of model efficiency and error estimation AIC have also applied in this comparative study.

From Table S_3 , it can be explained that the Freundlich model yielded the lowest χ^2 and AIC_c values for adsorption of anthocyanin and phenolics of both the sources on DIAION HP 20 resin whereas, Temkin and Langmuir models were also resulted lowest χ^2 and AIC_c values in adsorbing black rice anthocyanin on the same resin. For sugar adsorption of both the sources on the same resin, Elovich model proved best to explain. Similarly, in case of OPTIPORE L 493 resin, Freundlich model exhibited lowest χ^2 and AIC_c values for adsorption of both type of

anthocyanin. I this case also, sugar of both the sources didn't fitted any of the model well except Elovich model. According to the calculated error functions, it can be said that mostly Freundlich models is able to describe the sorption behavior of acylated or non-acylated anthocyanin and phenolics of respective sources onto both type of resins except sugars (Table S₄). Buran et al. [5] reported that Langmuir isotherm model can predict better way the adsorption mechanism of both anthocyanin and phenolics from blueberry extracts on resins. Adsorption behavior of flavonoids of oil palm on macroporous resin was well explained by Freundlich isotherm model [22]. None of the earlier reports were clear about the comparative adsorption between anthocyanin and phenolics. Whereas, Chen et al. [23] in their studies observed the adsorption mechanism of flavonoids on XAD-7HP and AB-8 resins follows Langmuir isotherm model. The flavonoids group present in the mulberry are quite smaller in size with similar energy distribution and

that is why mono layer adsorption pattern observed compared to anthocyanin.

3.5. Desorption study

Per cent desorption was very limited for both type of anthocyanin from both the resins (Table S_4). On the contrary, phenolics desorption is quite higher than anthocyanin from both type of resins. In case of acylated anthocyanin, phenolics get desorbed from DIAION HP 20 adsorbent resin 31 times higher than anthocyanin, whereas in case of non-acylated anthocyanin, phenolics get desorbed from DIAION HP 20 adsorbent resin 5 times higher than anthocyanin. The desorption of acylated and non-acylated anthocyanin from OPTIPORE L 493 resin is nil whereas corresponding phenolics somewhat get desorbed from ion exchange resin viz., 18.12~% of acylated source and 3.57~% of non-

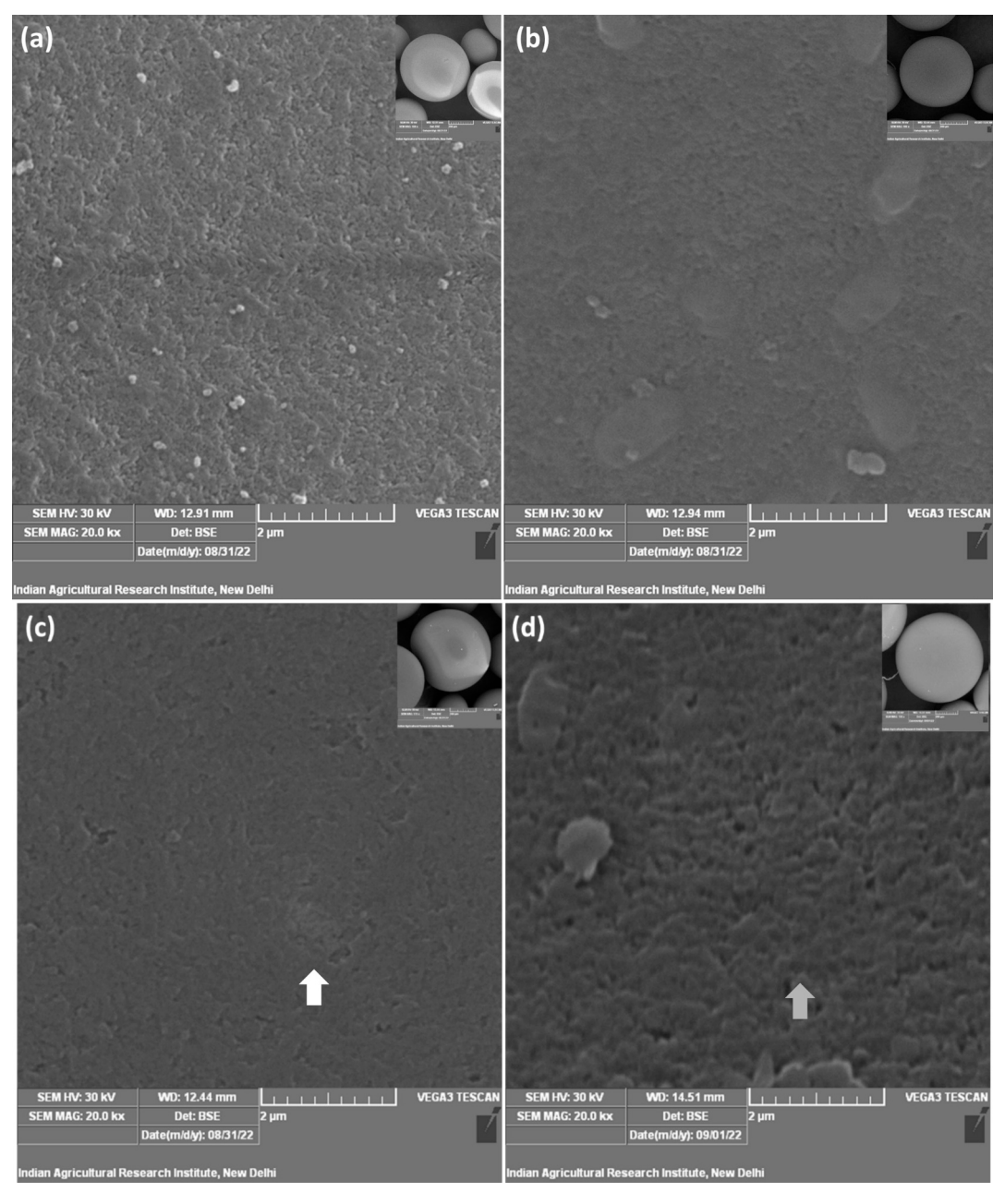


Fig. 1. Scanning electron micrographs (20 k magnification) for resins before and after adsorption (a) DIAION HP 20 resin (b) Anthocyanin adsorbed on DIAION HP 20 resin (c) OPTIPORE L 493 resin (d) Anthocyanin adsorbed on OPTIPORE L 493 resin. White and grey arrow depicts the smooth and uneven surface morphology, respectively.

acylated source. Comparative to anthocyanin and other phenolics, sugar desorption from DIAION HP 20 and OPTIPORE L 493 are higher for both type of anthocyanin. In case of acylated source sugar get desorbed about 56 % from DIAION HP 20 adsorbent resin whereas, sugars of nonacylated source get desorbed from the same resin of about 48.14 % Similarly, from OPTIPORE L 493 resin, sugars of non-acylated source get desorbed all most completely (92.16 %) than the acylated source (44.56 %). Although phenolics content is more in black rice and get more adsorbed by both type of resins but they get more desorbed from DIAION HP 20. On contrary, due to lesser phenolic content in black carrot, they get lesser adsorbed on OPTIPORE L 493 and desorbed too from the same resin as the bonding was not so strong. In nutshell, desorption was negligible phenomenon for anthocyanin from both the resins whereas desorption of phenolics and sugars were satisfactory good. Hence desorption is not an important criteria during selection of resins for anthocyanin purification. Lower desorption of anthocyanins is beneficial for the purification purpose. Lower the desorption in normal condition will lead to better purification. As the removal of adsorbed compounds mainly anthocyanins is done by solvent, lower desorption in aqueous condition generally helps in getting better purification. Mohammad et al. [24] reported that anthocyanins from grape skin get adsorbed on XAD-7HP quite strong (60.2 % adsorption) enough than the other phenolics and in contrast desorption was lesser. Hence, purification factor of anthocyanin increased to 41.88 although with the decrease of anthocyanin recovery Similarly, Yang et al. [25] reported that the adsorption capacity of DM21 is comparable good than desorption capacities. Hence, desorption is one of required parameter to correlate the adsorption capacities of anthocyanin, phenolics and sugars.

3.6. Characterization of macroporous resins

The SEM morphologies of macroporous resins were depicted before

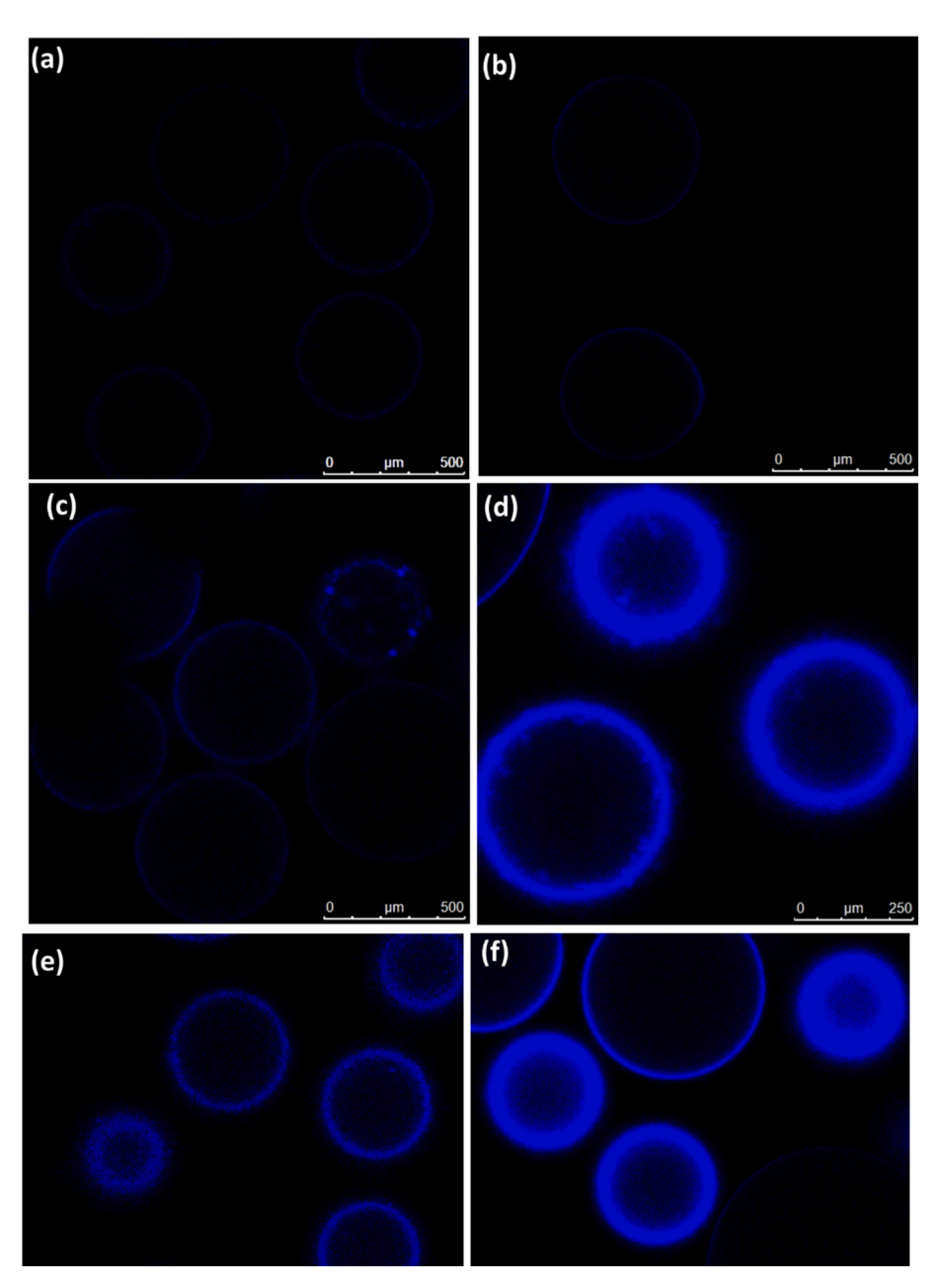


Fig. 2. Fluorescence microscopic images (excitation state at 413 nm and emission state at 550 nm) for (a) unadsorbed DIAION HP 20 resin, (b) unadsorbed OPTIPORE L 493 resin, non acylated anthocyanin of black rice extract adsorbed on (c) DIAION HP 20 resin (d) OPTIPORE L 493 resin, acylated anthocyanin of black carrot extract adsorbed on (e) DIAION HP 20 resin (f) OPTIPORE L 493 resin.

and after the adsorption process in Fig. 1. The SEM images reveal that prior to adsorption, all macroporous resins exhibited a cohesive spherical geometry, characterized by numerous micropores on the surface, contributing to their rough appearance. After adsorption there were some visible structural changes observed, notably there was a discernible reduction in the surface roughness of the macroporous resins. Similar observation noted by [26] surface of HPD-100 resin gets roughened with increasing power density of ultrasonication and thereby increased adsorption.

Adsorption of anthocyanin onto the resin particle surface was effectively demonstrated through confocal microscopic analysis. The detailed surface morphology of the resin particles was observed using this technique. Anthocyanins exhibit weak fluorescence when excited at a wavelength of 413 nm and emit at 594 nm. Leveraging this characteristic, confocal images of both unadsorbed and adsorbed resins were captured (Fig. 2). The resin particle boundaries displayed weak fluorescence (Fig. 2a and b). A distinct fluorescent band was observed on the surface of the adsorbed resin particles, although the fluorescence intensity varied depending on the specific anthocyanin. From the images (Fig. 2c and e), it can be visualized that in case of non-acylated anthocyanin of black rice sorption on DIAION HP 20, the resins get good coverage by black rice depending upon the emitted band. Whereas, for acylated one, the emitted band by black carrot extract is more than non acylated one as the coverage is comparative more and prominant than black rice. In case of OPTIPORE L 493, it is clearly distinguished that both type of anthocyanin got more adsorbed than DIAION-HP 20 (Fig. 2d and f). Above all, the emitted band of black carrot adsorbed ion exchange resin particles gave maximum among all tested resin particles. The novel, standalone confocal microscopy observations aligned closely with the earlier findings from the adsorption studies on both types of resins. By capturing images across the depth of the resin particles, confocal microscopy provided insights into the pore structure of the resins. This study marks the first instance where confocal microscopy has been utilized to elucidate and detail the mechanism of anthocyanin adsorption onto the surface of macroporous resin

The BET surface area of only DIAION HP 20, OPTIPORE L 493 are 486.15, 817.38 $m^2\ g^{-1}$ respectively. After adsorption of black rice and black carrot extract the surface area of DIAION HP 20 reduced to 77.50 and 146.96 $m^2\ g^{-1}$ respectively. Whereas in case of OPTIPORE L 493 resin, after adsorption of black rice extract the surface area reduced to 806.77 $m^2\ g^{-1}$ (Table S_5). It can be explained that after adsorption, the pore spaces of macroporous resin get reduced and thereby surface area also reduced. In previous study by Foo et al. [27], observed that nitrogen adsorption on oil palm fiber activated carbon was improved by microwave activation due to generation of higher surface area which is analyzed by BET (707.79 $m^2\ g^{-1}$).

3.7. Dynamic adsorption and validation of resin based purification study

Through dynamic adsorption study the purity improvement of nonacylated anthocyanins achieved between 43.9 and 44.1 %, whereas for acylated anthocyanins, it was 138.8–243.6 %. In a previous study, Chen et al. [23] reported that the purity of anthocyanin from mulberry was enriched to 93.6 % using XAD-7HP resin. Similarly, Yao et al. [28] achieved a 30.2 % increase in bilberry anthocyanin purity using XAD-7 resin, while Wu et al. [29] observed a 25 % enhancement in blueberry anthocyanin purity with the same type of resin. In present study, negligible co-extractive peaks in HPLC chromatogram exhibited the level of purification acquired by the method (Fig. S₄). The purity % is lesser in case of black rice can be due to comparative adsorption of other co extractives along with non acylated anthocyanin may play a key role during adsorption process. The purity percentage is highest for black carrot (243.6 %). It reassures that the acylated anthocyanin get more adsorbed than non-acylated one, on ion exchange resin.

Due to competitive adsorption of non-acylated anthocyanin and other phenolics, lesser purity was observed in case of anthocyanin extract belongs to non-acylated source (black rice). Whereas, there was comparatively lesser competition for the adsorbent site in the resin when acylation was there in the anthocyanin and that might be due to the size of the molecule, which gives advantage in terms of preferential adsorption through different bonds.

4. Conclusion

For the purpose of developing cost effective anthocyanin purification technology and its industrial utilization, standardization of adsorption method was done using both type of resin employing optimization of time, ratio (amount of resin: volume of extract), concentration, pH, temperature etc. All the previous studies were able to succeed in purity improvement of anthocyanin from wide varieties of sources, but none of the studies discussed about the differential behaviors of acylated and non-acylated anthocyanin at resin surface at wider dimension. Hence the present study stood out as the first ever study taking care of all probable aspects which influence the adsorption of acylated and nonacylated anthocyanin on macroporous resin surface. Standardized adsorption methodology for both acylated and non-acylated anthocyanin revealed that faster equilibrium was achieved by ion exchange resin. To achieve similar adsorption for both type of anthocyanins, 62.5 mg ion exchange resin was equivalent to 250 mg adsorbent resin. Freundlich model best explained the adsorption of all the four sources on both type of resins. Apart from anthocyanins, phenolics also followed same adsorption behavior but not sugars. It also confirmed that heterogeneous energy level exists at adsorbent-adsorbate surface. At optimized equilibrium time and ratio, at pH 3.0, acylated anthocyanin get adsorbed maximum whereas at pH 4.5 non-acylated anthocyanin adsorbed maximum on DIAION HP 20 resin. Whereas on OPTIPORE L 493 resin, at pH 4.5 and 6.0 acylated and non-acylated anthocyanin adsorbed maximum. At all studied temperatures, adsorption behavior was similar for both type of anthocyanins which is endothermic, spontaneous and random in nature. SEM and confocal microscopy was successfully used to monitor the anthocyanin adsorption process on macroporous resin surface. The study can be validated using more number of sources of anthocyanins for the confirmation of the result obtained in the present study. Similar result across sources further confirms the hypothesis.

OPTIPORE L 493 is the best resin in adsorbing acylated anthocyanin but not phenolics, whereas, in case of non acylated anthocyanin source, adsorption of both type of compounds were comparable. Moreover, on both the resins sugar get least adsorbed for both type of anthocyanin. Hence, OPTIPORE L 493 mediated anthocyanin purification technology holds promising efficiency and can be effectively applied to large scale production of anthocyanin purification in nutraceutical industry due to prominent advantages (procedural simplicity, low labor intensity, low cost etc.) and the greenness factors associated with it.

The present study reveals resin-specific selective adsorption of acylated versus non-acylated anthocyanins. It also combine SEM and confocal microscopy with rigorous isotherm selection (R², χ^2 , AICc) and thermodynamic analysis to provide mechanistic insight for improving anthocyanin purification.

CRediT authorship contribution statement

Anindita Paul: Writing – review & editing, Writing – original draft, Methodology, Investigation, Formal analysis, Data curation. Anirban Dutta: Writing – review & editing, Investigation, Formal analysis, Conceptualization. Aditi Kundu: Supervision, Software, Resources, Funding acquisition, Conceptualization. Namita Banyal: Visualization, Validation, Investigation. Gautam Chawla: Validation, Methodology, Data curation. Anil Dahuja: Writing – review & editing, Software, Resources, Methodology, Formal analysis. Supradip Saha: Writing – review & editing, Project administration, Funding acquisition, Conceptualization.

Consent for publication

Not applicable.

Declaration of generative AI and AI-assisted technologies in the writing process

During the preparation of this work the author(s) used ChatGPT in order to improve the language of the manuscript. After using this tool/service, the author(s) reviewed and edited the content as needed and take(s) full responsibility for the content of the publication.

Funding

The authors are thankful to ICAR-Indian Agricultural Research Institute, New Delhi-110012 and Department of Agricultural Research and Education, ICAR, New Delhi for financial assistance.

Declaration of competing interest

The authors declare that they have no known competing financial interests or personal relationships that could have appeared to influence the work reported in this paper.

Acknowledgments

Research was supported by the Indian Council of Agricultural Research, Department of Agricultural Research and Education, Government of India.

Ethics approval and consent to participate.

Not applicable.

Appendix A. Supplementary data

Supplementary data to this article can be found online at https://doi.org/10.1016/j.microc.2025.115976.

Data availability

Data will be made available on request.

References

- [1] S.M. Jafari, M.G. Ghalenoei, D. Dehnad, Influence of spray drying on water solubility index, apparent density, and anthocyanin content of pomegranate juice powder, Powder Technol. 311 (2017) 59–65.
- [2] I. Tontul, A. Topuz, Spray-drying of fruit and vegetable juices: effect of drying conditions on the product yield and physical properties, Trends Food Sci. Technol. 63 (2017) 91–102.
- [3] F. Sheng, Y. Wang, X. Zhao, N. Tian, H. Hu, P. Li, Separation and identification of anthocyanin extracted from mulberry fruit and the pigment binding properties toward human serum albumin, J. Agric. Food Chem. 62 (28) (2014) 6813–6819.
- [4] B. Smidova, D. Satínsky, K. Dostalova, P. Solich, The pentafluorophenyl stationary phase shows a unique separation efficiency for performing fast chromatography determination of highbush blueberry anthocyanins, Talanta 166 (2017) 249–254.

- [5] T.J. Buran, A.K. Sandhu, Z. Li, C.R. Rock, W.W. Yang, L. Gu, Adsorption/desorption characteristics and separation of anthocyanins and polyphenols from blueberries using macroporous adsorbent resins, J. Food Eng. 128 (2014) 167–173.
- [6] D. Kammerer, J. Gajdos Kljusuric, R. Carle, A. Schieber, Recovery of anthocyanins from grape pomace extracts (*Vitis vinifera L. cv. Cabernet Mitos*) using a polymeric adsorber resin, Eur. Food Res. Technol. 220 (3) (2005) 431–437.
- [7] Zaganiaris, E. J. (2019). Ion Exchange Resins and Synthetic Adsorbents in Food Processing. BoD-Books on Demand.
- [8] A.A. Zagorodni, Ion Exchange Materials: Properties and Applications, Elsevier, 2006
- [9] V. Camel, Solid phase extraction of trace elements. Spectrochimica Acta. Part B, At. Spectrosc. 58 (7) (2003) 1177–1233.
- [10] E. Sadilova, R. Carle, F.C. Stintzing, Thermal degradation of anthocyanins and its impact on color and in vitro antioxidant capacity, Mol. Nutr. Food Res. 51 (12) (2007) 1461-1471.
- [11] J. Bretag, D.R. Kammerer, U. Jensen, R. Carle, Adsorption of rutin onto a food-grade styrene-divinylbenzene copolymer in a model system, Food Chem. 114 (1) (2009) 151–160.
- [12] J. Bretag, D.R. Kammerer, U. Jensen, R. Carle, Evaluation of the adsorption behavior of flavonoids and phenolic acids onto a food-grade resin using a Doptimal design, Eur. Food Res. Technol. 228 (6) (2009) 985–999.
- [13] X.L. Chang, D. Wang, B.Y. Chen, Y.M. Feng, S.H. Wen, P.Y. Zhan, Adsorption and desorption properties of macroporous resins for anthocyanins from the calyx extract of roselle (*Hibiscus sabdariffa* L.), J. Agric. Food Chem. 60 (9) (2012) 2368–2376.
- [14] Y. Chen, D. Zhang, Adsorption kinetics, isotherm and thermodynamics studies of flavones from *Vaccinium Bracteatum* Thunb leaves on NKA-2 resin, Chem. Eng. J. 254 (2014) 579–585.
- [15] T. Belwal, L. Li, X. Yanqun, G. Cravotto, Z. Luo, Ultrasonic-assisted modifications of macroporous resin to improve anthocyanin purification from a *Pyrus communis* var. Starkrimson extract, Ultrason. Sonochem. 62 (2020) 104853.
- [16] L. Firdaous, B. Fertin, O. Khelissa, M. Dhainaut, N. Nedjar, G. Chataigné, L. Ouhoud, F. Lutin, P. Dhulster, Adsorptive removal of polyphenols from an alfalfa white proteins concentrate: adsorbent screening, adsorption kinetics and equilibrium study, Sep. Purif. Technol. 178 (2017) 29–39.
- [17] C. Lv, J. Yang, R. Liu, Q. Lu, Y. Ding, J. Zhang, J. Deng, A comparative study on the adsorption and desorption characteristics of flavonoids from honey by six resins, Food Chem. 268 (2018) 424–430.
- [18] A. Paul, A. Dutta, A. Kundu, A. Ghosh, G. Chawla, S. Saha, Adsorption-guided purification of rose petal anthocyanins, Biomass Convers. Biorefinery (2024), https://doi.org/10.1007/s13399-024-06331-5.
- [19] J. Singh, K. Sharma, S. Walia, S. Saha, Anthocyanin profiling method based on isocratic elution for comparable speed, reproducibility, and quantitation with gradient elution, Food Anal. Methods 10 (1) (2014) 118–128.
- [20] L. Rodriguez-Saona, M. Giusti, R. Wrolstad, Anthocyanin pigment composition of red-fleshed potatoes, J. Food Sci. 63 (1998) 457–465.
- [21] Y. Gong, J. Zhang, F. Gao, J. Zhou, Z. Xiang, C. Zhou, L. Wan, J. Chen, Structure features and in vitro hypoglycemic activities of polysaccharides from different species of Maidong, Carbohydr. Polym. 173 (2017) 215–222.
- [22] M.S. Che Zain, S.Y. Lee, C.Y. Teo, K. Shaari, Adsorption and desorption properties of total flavonoids from oil palm (*Elaeis guineensis* Jacq.) mature leaf on macroporous adsorption resins, Molecules 25 (4) (2020) 778.
- [23] Y. Chen, W. Zhang, T. Zhao, F. Li, M. Zhang, J. Li, Y. Zou, W. Wang, S.J. Cobbina, X. Wu, L. Yang, Adsorption properties of macroporous adsorbent resins for separation of anthocyanins from mulberry, Food Chem. 194 (2016) 712–722.
- [24] S.S. Mohammad, N. da Rocha Rodrigues, M.I.M. Barbosa, J.L.B. Junior, Useful separation and purification of anthocyanin compounds from grape skin pomace Alicante Bouschet using macroporous resins, J. Iran. Chem. Soc. (2022) 1–9.
- [25] D. Yang, M.M. Li, W.J. Wang, G.D. Zheng, Z.P. Yin, J.G. Chen, Q.F. Zhang, Separation and purification of anthocyanins from Roselle by macroporous resins, LWT 161 (2022) 113371.
- [26] Z. Luo, Z. Guo, T. Xiao, H. Liu, G. Su, Y. Zhao, Enrichment of total flavones and licochalcone a from licorice residues and its hypoglycemic activity, J. Chromatogr. B 1114 (2019) 134–145.
- [27] K.Y. Foo, B.H. Hameed, Microwave-assisted preparation of oil palm fiber activated carbon for methylene blue adsorption, Chem. Eng. J. 166 (2) (2011) 792–795.
- [28] L. Yao, N. Zhang, C. Wang, C. Wang, Highly selective separation and purification of anthocyanins from bilberry based on a macroporous polymeric adsorbent, J. Agric. Food Chem. 63 (13) (2015) 3543–3550.
- [29] Y. Wu, Y. Han, Y. Tao, S. Fan, D.T. Chu, X. Ye, M. Ye, G. Xie, Ultrasound assisted adsorption and desorption of blueberry anthocyanins using macroporous resins, Ultrason. Sonochem. 48 (2018) 311–320.